Supporting Information

Multiple Roles of Unconventional Heteroatom Dopants in Chalcogenide Thermoelectrics: The Influence of Nb on Transport and Defects in Bi_2Te_3

Xin Guo,[a,b] Cunyin Zhang,[a,†] Zhongyuan Liu,[a,†] Pan He,[a] Robert Szczęsny,[c] Fangjun Jin,[d] Wanqiang Liu,[a] and Duncan H. Gregory,**[b]*

[a.] School of Materials Science and Engineering; Engineering Research Center of Optoelectronic Functional Materials for Ministry of Education, Changchun University of Science and Technology, Changchun, 130022, China.

[b.] WestCHEM, School of Chemistry, University of Glasgow, Glasgow, G12 8QQ, UK.

[c.] Faculty of Chemistry, Nicolaus Copernicus University, Gagarina 7, 87-100 Toruń, Poland.

[d.] International Joint Research Center for Nanophotonics and Biophotonics, School of Science, Changchun University of Science and Technology, Changchun, 130022, China.

[†] Cunyin Zhang and Zhongyuan Liu contributed to this work equally.

*Corresponding author. E-mail: guoyml@126.com (Xin Guo)

** Corresponding author. E-mail: Duncan.Gregory@glasgow.ac.uk (Duncan H. Gregory)

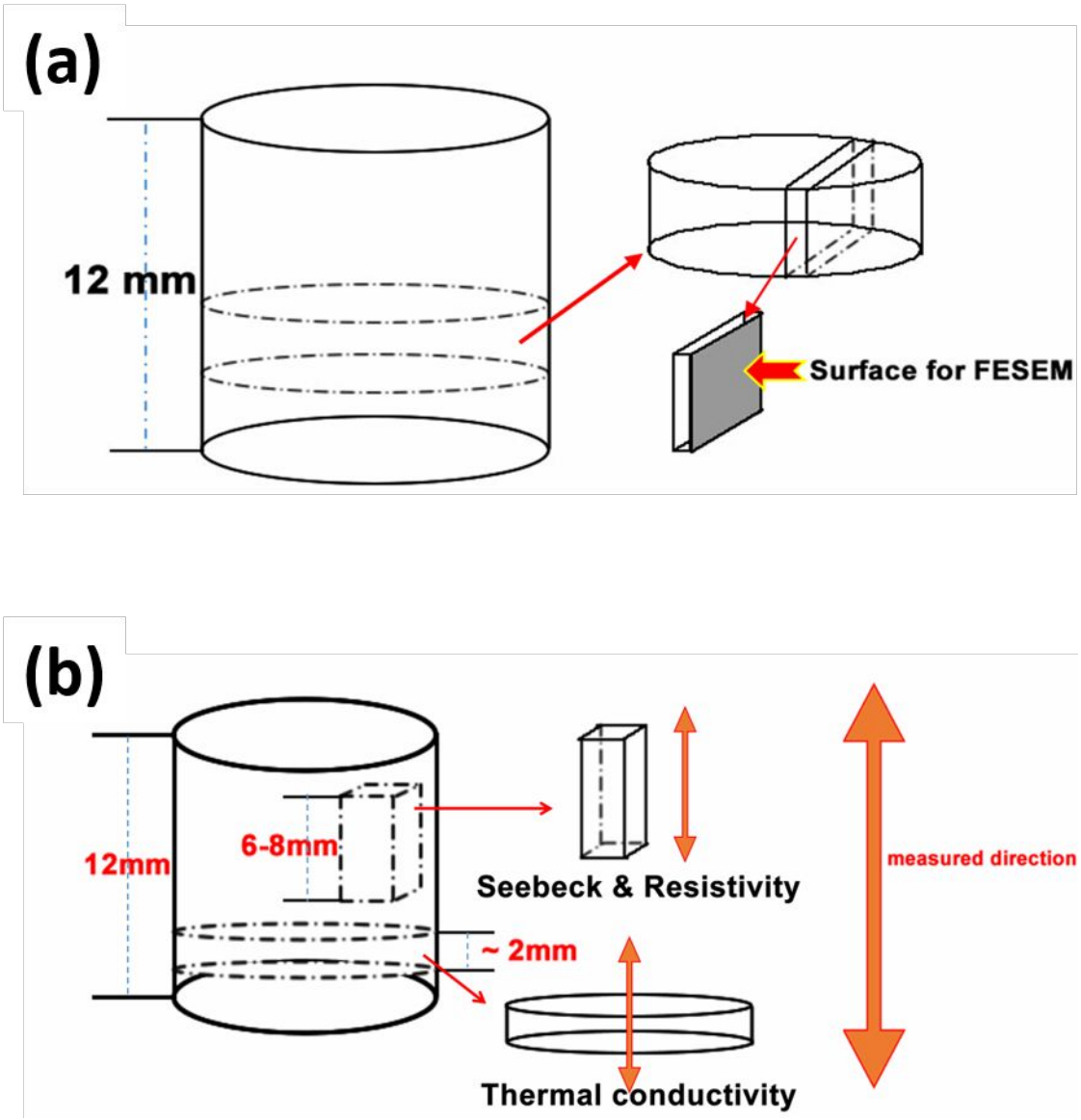

Figure S1. Schematics of the compact samples taken from the principal sample pellets as utilized for: (a) FESEM characterization experiments and (b) electrical and thermal property measurements.

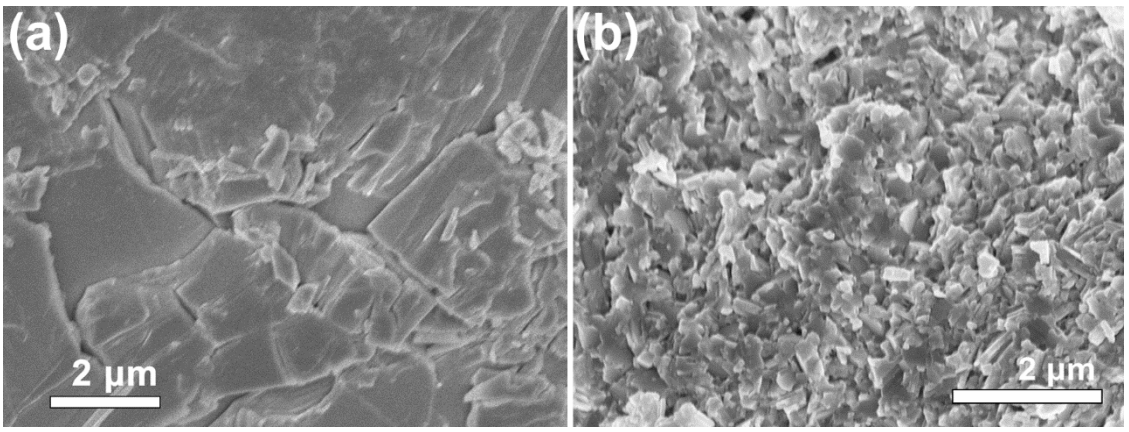

Figure S2. FESEM images of the fracture surface from (a) a Bi_2Te_3 pellet prepared (only) by the high-pressure sintering of the elemental powders and (b) $Bi_{1.92}Nb_{0.08}Te_3$ pellet vertical to the pressing direction.

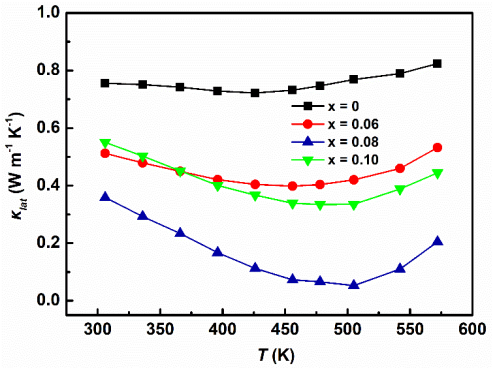

Figure S3. Temperature dependence of the lattice thermal conductivity for $Bi_{2-x}Nb_xTe_3$ (x = 0, 0.06, 0.08, 0.1).

Lattice thermal conductivity: The lattice thermal conductivity, as an indicator for estimating the effect of Nb doping on the phonon scattering, was calculated from total thermal conductivity subtracting electronic thermal conductivity, as shown in Figure S3. It is evident that the lattice thermal conductivity decreases significantly with increasing Nb content. Surprisingly, the $Bi_{2-x}Nb_xTe_3$ sample with x = 0.08 exhibits the ultralow lattice thermal conductivity compared with that of other samples over the measured temperature range. The ultralow lattice thermal conductivity seems to be lack of reasonability, especially for 425 – 550 K, which may be attributed to the unique synthesis method, high-pressure sintering (2 GPa). Hot pressing and SPS normally employ the sintering pressure that is around 80~100 MPa to be used to simply compress the sample powders, forming a compact pellet. As for pressure-sensitive Bi (~2.5 GPa will result in a phase transformation of Bi), ultrahigh pressure ~2 GPa may deeply influence some undefined mechanisms during the synthesis process of $(Bi,Nb)_2Te_3$, leading to the occurrence of ultralow lattice thermal conductivity. Saleemi *et al.* even reported a result that is the lattice thermal conductivity below zero in nanostructured Bi_2Te_3 bulk due to the overestimated Lorenz number (L) [(1)]. These findings above suggest that there must be some undefined mechanisms induced by specific synthesis method and structural modification, which will give rise to the inapplicability of the widely accepted L for special situation. However, this subject is out of our work in this article.

(1) M. Saleemi, M.S. Toprak, S.H. Li, M. Johnsson, M. Muhammed, *J. Mater. Chem.* 2012, 22, 725-730.

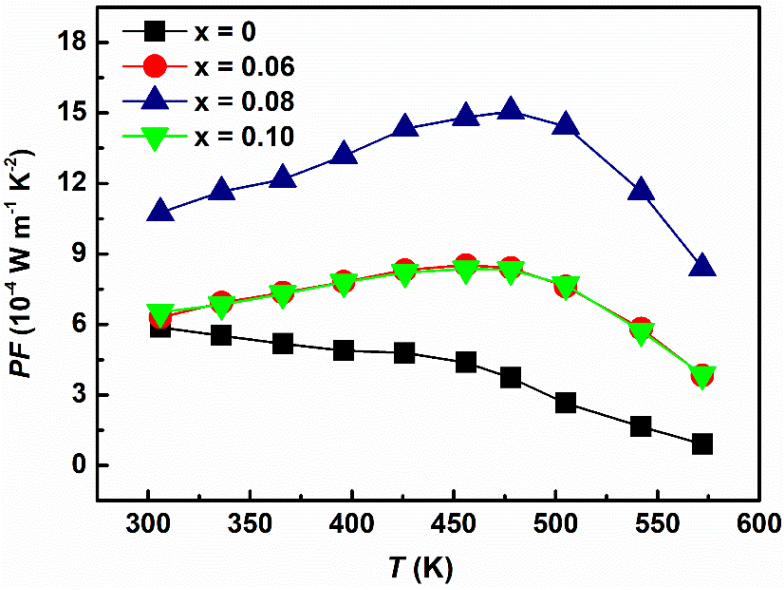

Figure S4. Temperature dependence of the power factor ($PF = S^2\sigma$) for $Bi_{2-x}Nb_xTe_{3-\delta}$ (x = 0, 0.06, 0.08, 0.1).

Power factor calculations: In order to evaluate the effect of Nb doping on the electrical transport properties of the Bi_2Te_3 system, the power factor was calculated using the values for the Seebeck coefficient and electrical conductivity discussed in the manuscript. As shown in Figure S3, a parabolic-like trend is observed for the temperature dependence of the power factors of the Nb-doped samples over the entire temperature range, which contrast markedly with the behavior of Bi_2Te_3. The data indicates that the maximum power factors for the Nb-containing Bi_2Te_3 samples shift to higher temperature, which is beneficial in terms of thermoelectric performance at high temperature. In addition, a significant enhancement in power factors is achieved for all the Nb-doped samples and is highest for the $Bi_{1.92}Nb_{0.08}Te_{3-\delta}$ sample. Hence, the increase in electrical conductivity more than compensates for the reduction in the Seebeck coefficient in each doped sample. The above results imply that, in the main, Nb-doping has a positive effect on the electrical transport properties in the Bi_2Te_3 system.

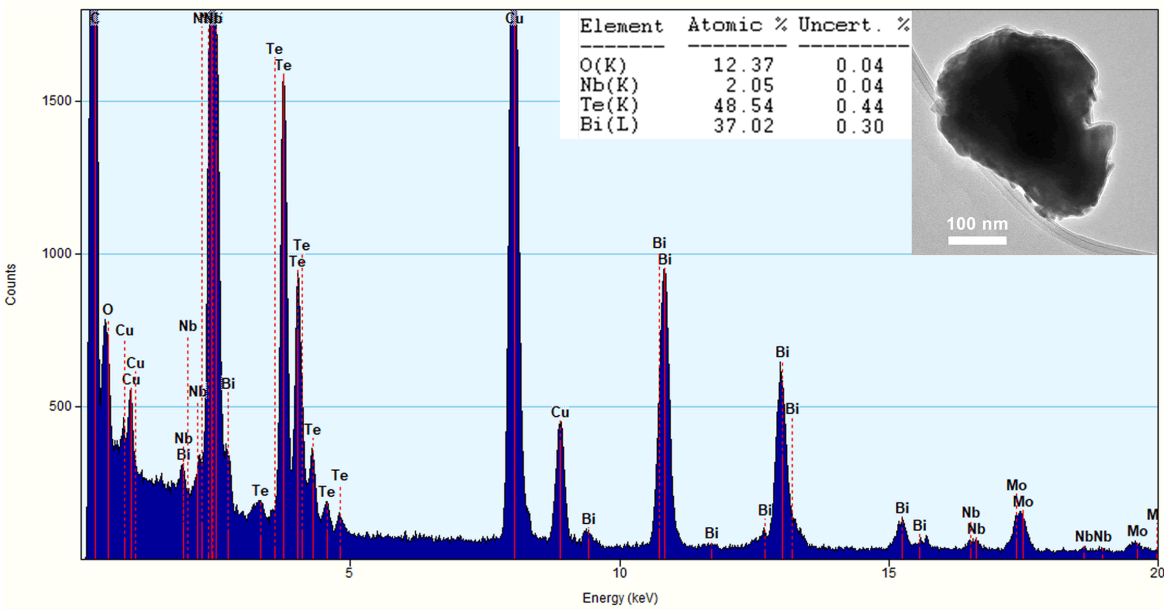

Figure S5. TEM-EDS spectrum taken from a single particle of $Bi_{1.92}Nb_{0.08}Te_{3-\delta}$. An image of the $Bi_{1.92}Nb_{0.08}Te_{3-\delta}$ particle is shown in the inset (top right). The derived elemental ratios are indicated in the second inset (top centre).

TEM/EDS measurements: The morphology and elemental composition of $Bi_{1.92}Nb_{0.08}Te_{3-\delta}$ sample was performed by a transmission electron microscope (FEI, G2 F20X-Twin 200 kV, FEG) equipped with energy-dispersive X-ray spectrometer (EDAX, RTEM model SN9577, 134 eV). Measurements were made in the TEM mode (bright-field) and the STEM mode (EDX). The dispersion of $Bi_{1.92}Nb_{0.08}Te_{3-\delta}$ sample was prepared in acetone by ultrasound and 5 µl of the solution was dropped on a TEM grid (carbon-coated copper mesh with holes; Lacey type Cu 400 mesh, Plano), and stored at room temperature until the solvent had completely evaporated. In addition to the expected peaks of Bi, Te and Nb in the EDS spectrum, peaks from the Cu grid and O from air exposure during handling prior to transfer to the TEM (and which grew slowly with exposure time) were noted.

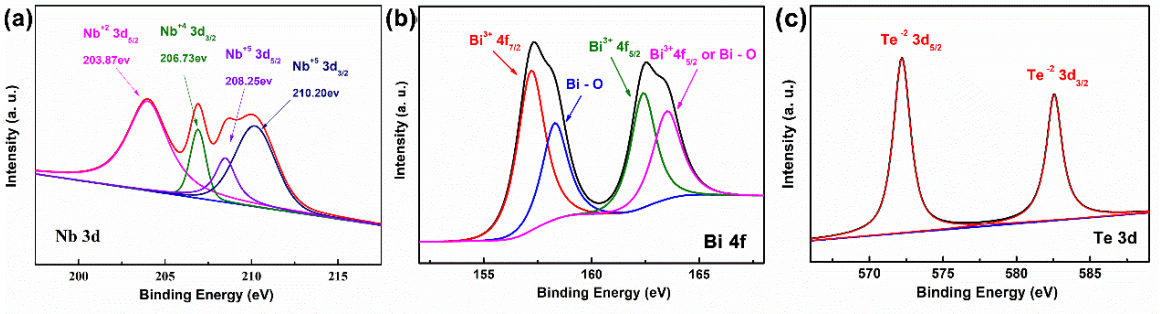

Figure S6. High-resolution X-ray photoelectron (XPS) spectra showing the corresponding binding energy regions for the: (a) Nb 3d, (b) Bi 4f, and (c) Te 3d peaks, respectively for the $Bi_{1.92}Nb_{0.08}Te_{3-\delta}$ sample. The respective Nb 3d, Bi 4f, and Te 3d bands were fitted to the relevant transitions and smoothed using the XPSPEAK 4.1 software package (R. W. M. Kwok, Chinese University of Hong Kong). The different peak positions and profiles at the binding energies of the Nb 3d, Bi 4f and Te 3d transitions were initially identified based on the NIST X-ray Photoelectron Spectroscopy Database (https://srdata.nist.gov/xps/Default.aspx) and references 31-33 in main article.

Table S1. The relative amount of the observed Nb species as taken from the Nb peaks in the XPS narrow scan spectrum shown in Figure S6(a) for $Bi_{1.92}Nb_{0.08}Te_{3-\delta}$.

Nb species	Nb^{+2} $3d_{5/2}$	Nb^{+4} $3d_{3/2}$	Nb^{+5} $3d_{5/2}$	Nb^{+5} $3d_{3/2}$
Relative amount	40.54 %	15.67 %	12.17 %	31.62 %